Biophysical Chemistry

Biophysical Chemistry 81 (1999) 157–178

www.elsevier.nl/locate/bpc

Review

Understanding mechanisms in a cooperative protein: the CO ligation intermediates of hemoglobin

Michele Perrella*

Dipartimento di Scienze e Tecnologie Biomediche, Università di Milano, L.I.T.A., Via F.lli Cervi, 93, I-20090 Segrate, Italy

Received 19 April 1999; received in revised form 6 July 1999; accepted 7 July 1999

Abstract

Hemoglobin is a regulatory component of the oxygen transport to the tissues, and for decades has been a prototype to develop new strategies for the study of the structure/function relationships in proteins. One of the most difficult, and so far, unattained objectives of hemoglobin research has been the study of the hemoglobin molecules in a state of partial ligation with oxygen, or intermediates, as a means of testing theories of cooperativity. A cryogenic technique has been developed for the isolation, identification and quantification of the reaction intermediates of hemoglobin and CO, which in many aspects is a close approximation to the physiological ligand. The technical features that are crucial for the evaluation of the significance of the experimental data obtained using this technique and various approaches to the analysis of the data are reported. The discussion points out the importance of accessing direct information on the nature and concentrations of the intermediates in solution to clarify mechanisms of cooperativity as opposed to the less informative studies of the bulk properties of the solution.

Keywords: Hemoglobin; Models of cooperativity; Cryofocusing; Reaction intermediates

1. Introduction

The Nobel prize awarded to Kendrew and Perutz in 1962 for the determination of the crystal structures of myoglobin and hemoglobin was a landmark event that determined the development of modern protein science. Since then, these proteins have been model compounds for the development of new technologies and theories for the study of the relationships between structure and function [1,2]. Myoglobin has a tertiary structure similar to that of the α and β chains in tetrameric, $\alpha_2\beta_2$, hemoglobin. The functional behaviour of myoglobin and of the isolated hemoglobin chains is characterised by a hyperbolic

---

* Tel.: +39-02-26423-303; fax: +39-02-264-233-02.

PII: S0301-4622(99)00093-9

oxygen binding isotherm with a P_{50} value of approximately 1 torr, which makes this protein inadequate for oxygen transport. Assembling two α and two β chains in a tetramer brings about a dramatic change in function. The sigmoidal shape of the oxygen binding isotherm of hemoglobin allows the protein to load oxygen at the lungs, where the ligand concentration is high, and to unload it at the tissues, where the ligand concentration is low. The P_{50} value, which under physiological conditions is approximately 28 torr, shifts with the change in binding of several allosteric ligands, such as hydrogen ions, chloride, carbonic anhydride and 2,3-biphosphoglycerate (2,3-BPG),

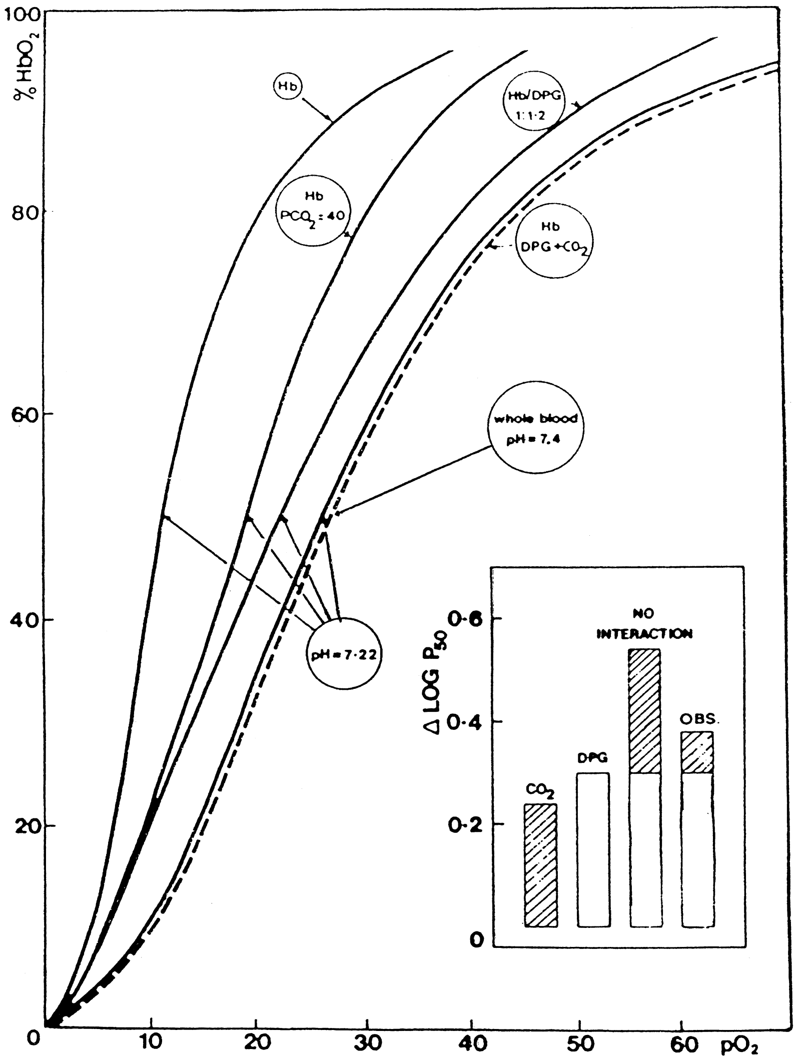

Fig. 1. Oxygen equilibrium isotherms at 37°. Full curves, hemoglobin solutions in 0.1 M KCl, pH 7.22, equilibrated with (from left to right): O_2/N_2 mixtures; $O_2/N_2/CO_2$ mixtures ($P_{CO_2} = 40$ torr); O_2/N_2 mixtures and a slight molar excess of 2,3-BPG; $O_2/N_2/CO_2$ mixtures ($P_{CO_2} = 40$ torr) and a slight molar excess of 2,3-BPG. Dashed curve: fresh whole blood equilibrated with $O_2/N_2/CO_2$ mixtures ($P_{CO_2} = 40$ torr) at pH 7.4. Inset (from left to right), increments in $\log P_{50}$ observed by the single additions of CO_2 and 2,3-BPG, increment calculated by summing the single effects of CO_2 and 2,3-BPG and increment observed by the addition of both CO_2 and 2,3-BPG. Adapted from Brenna et al. [4].

(Fig. 1). The affinities of the modulators for the binding sites, distant from the hemes, are higher in the unliganded state of the protein and are modified by the binding of the other modulators. A body of information unique in its richness has been gathered on the kinetic, thermodynamic and structural properties of the liganded and unliganded forms of the protein and on their interactions with the modulators. In some cases the nature of the interactions among some of the modulators has been clarified, as shown by the studies on blood gas transport by Rossi-Bernardi and collaborators [3,4]. They demonstrated that the oxygen binding isotherm of whole blood under physiological conditions of CO_2, 2,3-BPG and hydrogen ion concentrations is reproduced in vitro by the addition of the physiological concentrations of these modulators to concentrated solutions of hemoglobin in 0.1 M KCl. The effects of CO_2 and 2,3-BPG, however, are not additive, indicating competitive interactions with the protein (Fig. 1).

Most of the experimental evidence on the mechanisms of the interactions between the hemoglobin and oxygen and the modulation of such interactions has been provided so far by the analyses of the oxygen binding isotherms. These data together with the information on the structural and functional properties of the end states, i.e. oxy- (HbO_2) and deoxyhemoglobin (Hb), have provided a great deal of the experimental support for the most successful model for the interpretation of cooperativity, which was described by Monod et al. 1965 [5]. The MWC model assumes that at each stage of the ligation process the protein molecules exist in equilibrium between two structures. Structure T, identified with the structure of the crystals of Hb, has low affinity for oxygen. Structure R, identified with the structure of the crystals of methemoglobin (Hb^+) and carboxyhemoglobin (HbCO) has high affinity for the ligand. Cooperativity ensues from the progressive increase in the proportion of molecules in the R structure driven by the increase in bound ligands according to the law of mass action. The tertiary changes in the structure of the subunits, which must occur on ligation, do not contribute to cooperativity. An alternative model (KNF), described by Koshland et al. [6] in 1966, does not assume a pre-existing equilibrium of structures. The structure of the cooperative molecule switches progressively from the T to the R configuration according to the rules of subunit interactions in the course of ligation specific to that molecule. Cooperativity ensues from the tertiary structural changes. Information on the functional and structural properties of the intermediate states of ligation or on the distributions of such species under a particular set of conditions, although not required to define the MWC model, is nevertheless the ultimate test for both the MWC and KNF models.

The aim of this article is to give an account of the work carried out to isolate, identify and quantify the partially liganded species, intermediates in short, in the reactions of hemoglobin with carbon monoxide. The intermediates are rare species in the sense that they are unstable and their concentrations are low, particularly under equilibrium conditions. The results of this 20-year long effort point out how essential the information on these species is for the clarification of the mechanisms of cooperativity. The key methodology that made the project possible is a cryogenic electrophoretic technique for the separation of protein species stabilised at low temperatures. Hopefully this article will provide the background for a proper evaluation of the work carried out so far, progress and pitfalls, and contribute to diffuse the information on the cryogenic technique, which may prove useful in the study of other systems involving unstable species, such as protein–protein, protein–peptide and protein–nucleic acid complexes.

2. Trapping the intermediates

2.1. Background

The α and β chains assembled in the hemoglobin oxy- and deoxytetramer form two types of contacts. The $\alpha_1\beta_1$ and the symmetrical $\alpha_2\beta_2$ contacts are extensive and do not dissociate under physiological conditions. The $\alpha_1\beta_2$ and the symmetrical $\alpha_2\beta_1$ contacts dissociate yielding two structurally identical dimers, $\alpha_1\beta_1$ and $\alpha_2\beta_2$. Because of the non-equivalence of α/β contacts and the assumed intrinsic differences in the properties of the α and β chains, the binding of heme ligands yields 10 ligation states, as depicted in Fig. 2. In solutions of partially liganded ferrous hemoglobin all the states are unstable because of: (a) the mobility of the ligand, which can dissociate from a heme and rebind to a different heme; and (b) the exchange of dimers among the tetramers according to the scheme in Fig. 3. All three gaseous ligands, O_2, CO and NO, have high rates for the association reaction. The rate of the dissociation reaction, the step controlling the mobility of the ligand, is markedly different for the three ligands. Oxygen and nitric oxide have the highest and slowest dissociation rates, respectively and similar association rates [7]. Carbon monoxide is an intermediate case with a value of the dissociation rate constant of approximately 0.01 s^{-1} from HbCO and 0.1 s^{-1} from the monoliganded species [8]. Contrary to NO, CO equilibrium isotherms similar to the oxygen isotherms have been measured [9,10].

As shown by the work of Ackers and collaborators [11], the dimer association reaction is fast and independent of the type of ligand and state of ligation of the associating dimers, whilst the tetramer dissociation is strongly dependent on both the ligand and state of ligation of the tetramer. Therefore the controlling step of the dimer rearrangement reactions is the tetramer dissociation reaction.

2.2. *Cryomethods and the strategy for the isolation of the intermediates*

The project for trapping the intermediates between hemoglobin and CO was inspired by Rossi-Bernardi who suggested that the difference

$(\alpha\beta)\,(\alpha\beta)$
[01]

$(\alpha^{co}\beta)\,(\alpha\beta)$ [11]
$(\alpha\beta^{co})\,(\alpha\beta)$ [12]

$(\alpha^{co}\beta^{co})\,(\alpha\beta)$ [21]
$(\alpha^{co}\beta)\,(\alpha\beta^{co})$ [22]
$(\alpha^{co}\beta)\,(\alpha^{co}\beta)$ [23]
$(\alpha\beta^{co})\,(\alpha\beta^{co})$ [24]

$(\alpha^{co}\beta^{co})\,(\alpha^{co}\beta)$ [31]
$(\alpha^{co}\beta^{co})\,(\alpha\beta^{co})$ [32]

$(\alpha^{co}\beta^{co})\,(\alpha^{co}\beta^{co})$
[41]

Fig. 2. The 10 CO ligation states of hemoglobin. Each tetrameric species dissociates yielding the dimers, $(\alpha_1\beta_1)$ and $(\alpha_2\beta_2)$, shown in parentheses, where the subscripts are omitted for simplicity. In brackets is the notation of the *i*th ligation state and the respective degeneracy *j* according to Ackers [11].

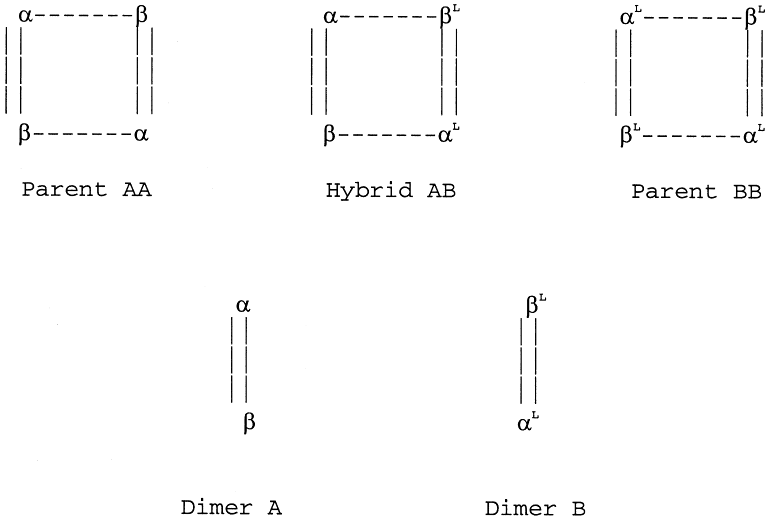

Fig. 3. Scheme of the dimer exchange reactions. The dashed lines indicate the $\alpha_1\beta_2$ and $\alpha_2\beta_1$ contacts that dissociate under physiological conditions. Each symmetrical parent species dissociates into dimers in the same ligation state. The asymmetrical hybrid dissociates into dimers in different state of ligation. Through the dissociation into dimers two parent tetramers in solution yield the hybrid and the hybrid disproportionates into the parent tetramers.

in the rate of oxidation by ferricyanide between the unliganded and the CO-liganded chains could be exploited to prevent the mobility of the ligand, since only the ferrous hemes bind CO. Furthermore, the oxidation of the heme iron would place a positive charge on each of the oxidised chains. Because of the different pK values of the α and β chains in the reaction:

$$\mathrm{Hb}^+ + \mathrm{H_2O} \rightarrow \mathrm{Hb}^+\mathrm{OH}^- + \mathrm{H}^+ \qquad (1)$$

the oxidation of the intermediates in Fig. 2 yields nine differently charged species. Species $(\alpha^+\beta^{\mathrm{CO}})(\alpha^{\mathrm{CO}}\beta^+)$ and $(\alpha^{\mathrm{CO}}\beta^{\mathrm{CO}})(\alpha^+\beta^+)$ cannot be distinguished. The nine species can be separated by chromatographic or electrophoretic methods, provided that some means of stabilising the tetramers is found. The pioneer work of Douzou and collaborators [12] in the field of cryobiochemistry provided useful information on the stability of the hemoglobin–carbon monoxide bond in hydro-organic solvents at subzero temperature. Furthermore, Park in 1975 showed that the asymmetrical valence hybrids of hemoglobin can be isolated by isoelectricfocusing (IEF) at subzero temperatures in the range from -5 to -10°C using gels of polyacrylamide, cross-linked with methylene-bis-acrylamide, in ethylene glycol/water mixtures containing Ampholines in the 6–8 pH range [13]. These important experiments helped define the proper strategy for the isolation of the CO intermediates. (1) Quenching a hemoglobin solution partially saturated with CO into an anaerobic hydro-organic solvent at subzero temperature containing an excess of ferricyanide would: (a) oxidise the unliganded chains to the ferric state; (b) prevent any dissociated ligand from rebinding to other chains; and (c) stabilise the ligand–hemoglobin interaction and prevent the oxidation of the liganded chains. (2) Cryofocusing the products of the chemical/thermal quenching would isolate nine out the 10 ligation states. The crucial steps in the procedure were the long-term stability at subzero temperatures, the resolution, identification, quantification of the oxidised intermediates and adequate validation tests, as described in the following.

2.3. Stability of the asymmetric species

At the moderate subzero temperatures attained by Park's technique the tetrameric species are not

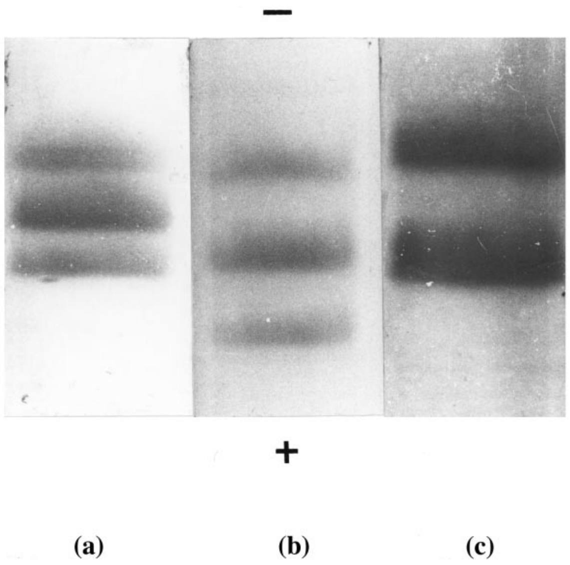

Fig. 4. Electrophoretic separations at −40° in 50% (v/v) Me_2SO. (a) Equimolar mixture of HbA(CO) and HbC(CO) incubated at 5°C for 15 min before separation for 2 h. (b) Same as (a), but after the separation in the three bands electrophoresis was interrupted for 2 h and then resumed for another 2-h period. (c) Samples of HbA(CO) and HbC(CO) mixed at −30° and then separated at −40°. Adapted from Perrella et al. [16].

stable enough over the long periods of time required to attain the focusing equilibrium in a highly viscous solvent. In less viscous solvents, such as mixtures of ethylene glycol/methanol/water, the polyacrylamide gels undergo a structural change, the glass transition, which makes them non-permeable to ions at just a few degrees below zero. Co-polymers of acrylamide, methylacrylate (or ethylacrylate) and methylene-bis-acrylamide have low glass transition temperatures in various hydro-organic solvents [14,15]. Using a standard thermostattable cell for gel tube electrophoresis, a simple modification of the standard buffers for discontinuous buffer gel electrophoresis, consisting of the dilution of the buffers and the addition of dimethylsulfoxide (Me_2SO) to 50% (v/v), good resolution of mixtures of HbA(CO), HbC(CO) and their hybrid, formed by dimer exchange at 5°C, was achieved in approximately 2 h of electrophoresis at −40°C, as shown in Fig. 4. Since at this temperature the asymmetrical hybrid species was stable for the time required for the separation, the amount of hybrid formed upon incubation of the parental species under various conditions of pH and temperature was quantified after separation and the rate constants for the tetramer dissociation reaction were calculated. These experiments indicated that the asymmetrical species would not exchange dimers significantly for periods of time of 20–30 h at temperatures ≤ -25°C and under alkaline pH conditions [16].

Subzero temperature electrophoresis is a valuable technique for the separation of species differing significantly in charge, which need to be stabilised at very low temperatures. The glass transition temperature of the co-polymer gels can be lowered by increasing either the proportion of methylacrylate or the length of the hydrocarbon chain of the alcoholic moiety of the ester. The second approach is of limited application since the solubility in hydro-organic solvents of the acrylate esters drops dramatically from methylacrylate to buthylacrylate. Nevertheless electrophoresis close to −50° is feasible using the methylacrylate/acrylamide co-polymers.

2.4. Separation of the valence hybrids by IEF

Electrophoresis is not suitable for the separation of the complex mixtures of partially oxidised HbCO, which were the objective of the project, since the positive charge of the oxidised chains is partially neutralised by Reaction 1. Good resolution is achieved by IEF using the acrylate ester/acrylamide co-polymers provided that the solutions of soda (catholite) and phosphoric acid (anolite) are replaced by Ampholine solutions. The subzero pH gradients, the time required for the attainment of such gradients and their time stability were measured using various mixtures of commercial Ampholines [17]. Shallow pH gradients, such as those shown in Fig. 5, allow the separation of nine species within 0.1 units of the pH gradient and 12–14 mm of gel length, although the complete resolution of all the species under these conditions also depends on the thickness of the protein zones [18].

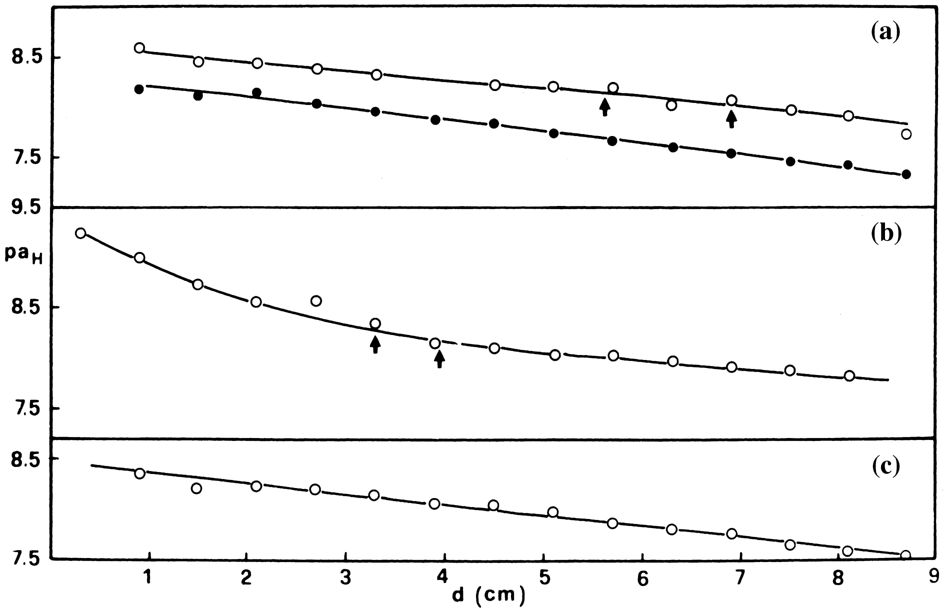

Fig. 5. pH gradients in tube gel IEF in 20% (v/v) ethylene glycol-15% (v/v) methanol-65% (v/v) water measured at subzero temperatures. (a) Gradients at −12°. ○, 1% Ampholine, pH 8–9.5, as catholite, 0.1% Ampholine, pH 6–8, as anolite, 3% Ampholine, pH 6–8, in the gel. Arrows show the positions reached in the gel by Hb^+ and HbCO after 24-h focusing. ●, 1% Ampholine, pH 7–9, as catholite, 0.1% Ampholine, pH 5–7, as anolite, 3% Ampholine, pH 5–7, in the gel. (b) Gradients at −23°. Ampholine ranges as in a (○). (c) Gradient at −23°. 1% Ampholine, pH 7–9, as catholite, 0.1% Ampholine, pH 6–8, as anolite, 3% Ampholine, pH 6–8, in the gel. Adapted from Perrella et al. [18].

2.5. Identification of the intermediates

A spectroscopic analysis of zones that, although sharp and resolved at subzero temperature, become distorted and slowly diffuse into one another upon exposure to room temperature is technically difficult per se. This approach would not solve the problem of species identification since the spectra of the oxidised chains are influenced in different ways by the pH and solvent composition of the gel zone in which each species focuses. The key to the solution of this problem is provided by the mechanism of the dimer exchange reactions, as shown in Fig. 6. A sample of partially oxidised HbCO, quenched into the cryosolvent and focused at −25°, yields a pattern of nine components, Fig. 6a. The same aqueous sample focused at 5° is resolved into four zones containing, from cathode to anode: Hb^+, $(\alpha^+\beta^{CO})(\alpha^+\beta^{CO})$, $(\alpha^{CO}\beta^+(\alpha^{CO}\beta^+)$, HBCO, Fig. 6b. The continuous disproportion at 5° of the asymmetrical hybrids, stable at −25°, causes segregation of the four symmetrical parental species. Since the charge of each hybrid species is the average charge of the respective parental species, in a linear pH gradient, such as the gradient in Fig. 5, the focusing zone of the hybrid is equidistant from the focusing zones of the parents [18]. The identification of the hybrids in Fig. 6a becomes straightforward when the identity of the parents is known.

As mentioned, intermediates $(\alpha^{CO}\beta^{CO})(\alpha\beta)$ and $(\alpha^{CO}\beta)(\alpha\beta^{CO})$ cannot be resolved since the oxidised counterparts have identical isoelectric points. The mechanism of the dimer exchange reactions again provides the key to the solution of the problem. Each hybrid species is stable at subzero temperature, but readily disproportionates into the parental species at temperatures above zero. If the zone on the gel containing the unresolved components, component no. 5 in Fig. 6a, is excised and the protein content is re-focused at 5°, the expected hemoglobin species are: (1) Hb^+ and HbCO, if the component contains

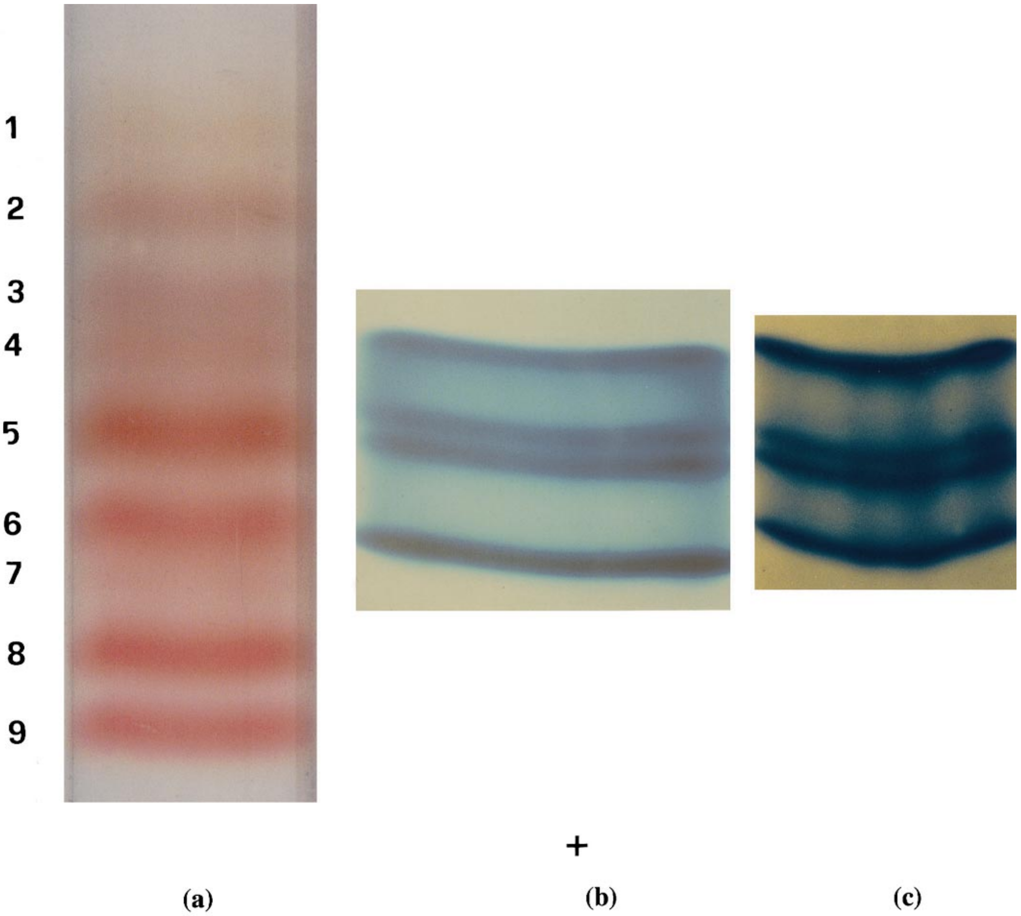

Fig. 6. Identification of the valence hybrids. (a) Pattern of nine components obtained by focusing a sample of 37%-oxidised HbCO at −25°. Components 1, 3, 7 and 9 are the symmetrical parents Hb^+, $(\alpha^+\beta^{CO})(\alpha^+\beta^{CO})$, $(\alpha^{CO}\beta^+)(\alpha^{CO}\beta^+)$ and HbCO, respectively; 2 is $(\alpha^+\beta^{CO})(\alpha^+\beta^+)$, hybrid of 1 and 3; 4 is $(\alpha^{CO}\beta^+)(\alpha^+\beta^+)$, hybrid of 1 and 7; 5 is the unresolved mixture of $(\alpha^{CO}\beta^{CO})(\alpha^+\beta^+)$ and $(\alpha^{CO}\beta^+)(\alpha^+\beta^{CO})$, hybrids of 1 and 9, 3 and 7, respectively; 6 is $(\alpha^+\beta^{CO})(\alpha^{CO}\beta^{CO})$, hybrid of 3 and 9; 8 is $(\alpha^{CO}\beta^+)(\alpha^{CO}\beta^{CO})$, hybrid of 7 and 9. (b) The four parental species (from cathode to anode: Hb^+, $(\alpha^+\beta^{CO})(\alpha^+\beta^{CO})$, $(\alpha^{CO}\beta^+)(\alpha^{CO}\beta^+)$ and HbCO) obtained by focusing on a gel plate at 5° the same sample as in (a). The separated proteins were stained with Coomassie Blue. (c) Disproportionation and separation by IEF at 5°, as parent species, of the hybrids isolated as component 5 in (a). The identification of all the asymmetrical hybrids in (a) was confirmed similarly by disproportionation [19].

species $(\alpha^{CO}\beta^{CO})(\alpha^+\beta^+)$; (2) $(\alpha^+\beta^{CO})(\alpha^+\beta^{CO})$ and $(\alpha^{CO}\beta^+)(\alpha^{CO}\beta^+)$, if the component contains species $(\alpha^{CO}\beta^+)(\alpha^+\beta^{CO})$; and (3) Hb^+, HbCO, $(\alpha^+\beta^{CO})(\alpha^+\beta^{CO})$ and $(\alpha^{CO}\beta^+)(\alpha^{CO}\beta^+)$, if the component contains both species. The relative amounts of Hb^+ plus HbCO and $(\alpha^+\beta^{CO})(\alpha^+\beta^{CO})$ plus $(\alpha^{CO}\beta^+)(\alpha^{CO}\beta^+)$ measure the relative concentrations of intermediates $(\alpha^{CO}\beta^{CO})(\alpha\beta)$ and $(\alpha^{CO}\beta)(\alpha\beta^{CO})$ in the quenched hemoglobin solution [19]. Fig. 6c is the analysis of component 5 in Fig. 6a by the above procedure indicating that component 5 is a mixture of $(\alpha^{CO}\beta^{CO})(\alpha\beta)$ and $(\alpha^{CO}\beta)(\alpha\beta^{CO})$.

2.6. Quantification of the intermediates

The concentrations of some intermediates under equilibrium conditions are less than 1% of the total and the gel zone comprising one such intermediate contains < 2 μg of protein under usual experimental conditions. The relative proportions of the focused components can be determined by densitometry of the zones using the gels still encased in the glass tubes [20] or using magnified colour slides of the gels [21]. In the first case resolution is impaired by diffusion of the zones during the procedure of tube alignment and calibration. In the second case the problem of diffusion is minimised by taking the slides immediately after removing the tubes from the electrophoresis cell, but the photographic procedure alters the spectral properties of the zones. In both cases a calibration procedure is required. Major problems were: low sensitivity; deconvolution of the peaks of irregular shape; base-line setting; and blank correction. An alternative to densitometry is the assay of the hemeproteins eluted from the gel slices containing the focused zones by the pyridine hemochromogen method [21]. The two methods were found comparable in precision using solutions of partially oxidised HbCO containing various and large proportions of ferric and ferrous chains [21]. The pyridine hemochromogen method does not require calibration, is sensitive and suitable for determining the low amounts of protein isolated in the equilibrium experiments. Blanks carried out using samples of pure Hb and HbCO (see Fig. 10) allow the optimisation of the quenching conditions and the estimation of corrections, when necessary. The error due to contamination of a protein zone by the adjacent zones during gel slicing is averaged out by eluting several slices containing the same zone. The fractions of the nine species isolated from samples of hemoglobin equilibrated with CO in five independent experiments at 48% saturation and the errors are listed in Table 1 to provide an example of the application of the method. The method yielded a similar percent error in the 15–85% CO saturation range.

2.7. Validation of the procedure

Each step of the chemical/thermal quenching procedure for trapping the CO intermediates has been tested [21]. However, before any attempt to use data to study function, a test for the whole procedure was needed that would make it reliably applicable under the conditions of paucity of intermediates due to cooperativity. The following experiments describe the problem and the answer provided.

Fig. 7a–d are scans of colour slides of gel tubes showing the formation of the intermediates during the approach to equilibrium in solutions of Hb and HbCO rapidly mixed in 1:1 ratio and reacted for times varying from 50 ms to 15 min before quenching [22]. The concentrations of the intermediates build up through the reactions of dissociation and association of the ligand and the overall rate of the process were governed by the slowest reaction, i.e. the dissociation of CO from HbCO ($t_{1/2} \approx 7$ s). The total fractions of the intermediates, f_T, vs. time were: $t = 1.2$ s, $f_T =$

Table 1
Concentrations of CO intermediates at 48% saturation[a]

Species	Fraction (%)	Parameters
$(\alpha\beta)(\alpha\beta)$	41.8 ± 0.2	$K_\alpha = 1.5 \pm 0.1$ torr^{-1}
$(\alpha^{CO}\beta)(\alpha\beta)$	2.4 ± 0.1	$\mathrm{K}_\beta = 3.1 \pm 0.3$ torr^{-1}
$(\alpha\beta^{CO})(\alpha\beta)$	4.9 ± 0.3	$c_{\alpha\alpha} = 29 \pm 4$
$(\alpha^{CO}\beta)(\alpha^{CO}\beta)$	1.0 ± 0.1	$c_{\alpha\beta} + \mathrm{c}_{\alpha\beta} = 21 \pm 4$
$(\alpha^{CO}\beta)(\alpha\beta^{CO})$	2.9 ± 0.2	$c_{\beta\beta} = 10 \pm 2$
$+(\alpha^{CO}\beta^{CO})(\alpha\beta)$		$c_{\alpha\alpha\beta} = 942 \pm 186$
$(\alpha\beta^{CO})(\alpha\beta^{CO})$	1.4 ± 0.2	$c_{\alpha\beta\beta} = 570 \pm 108$
$(\alpha^{CO}\beta)(\alpha^{CO}\beta^{CO})$	3.8 ± 0.5	$c_{\alpha\alpha\beta\beta} = 3.1 \times 10^5 \pm 0.7 \times 10^5$
$(\alpha\beta^{CO})(\alpha^{CO}\beta^{CO})$	4.7 ± 0.7	
$(\alpha^{CO}\beta^{CO})(\alpha^{CO}\beta^{CO})$	37 ± 2	

[a] Concentrations of CO intermediates at 48% saturation were obtained by equilibrating for 20 h at 20° in a gas tight syringe equimolar solutions of HbA and HbA(CO) in 0.1 M KCl, pH 7 ([23]). The site-specific parameters were calculated by Di Cera [30].

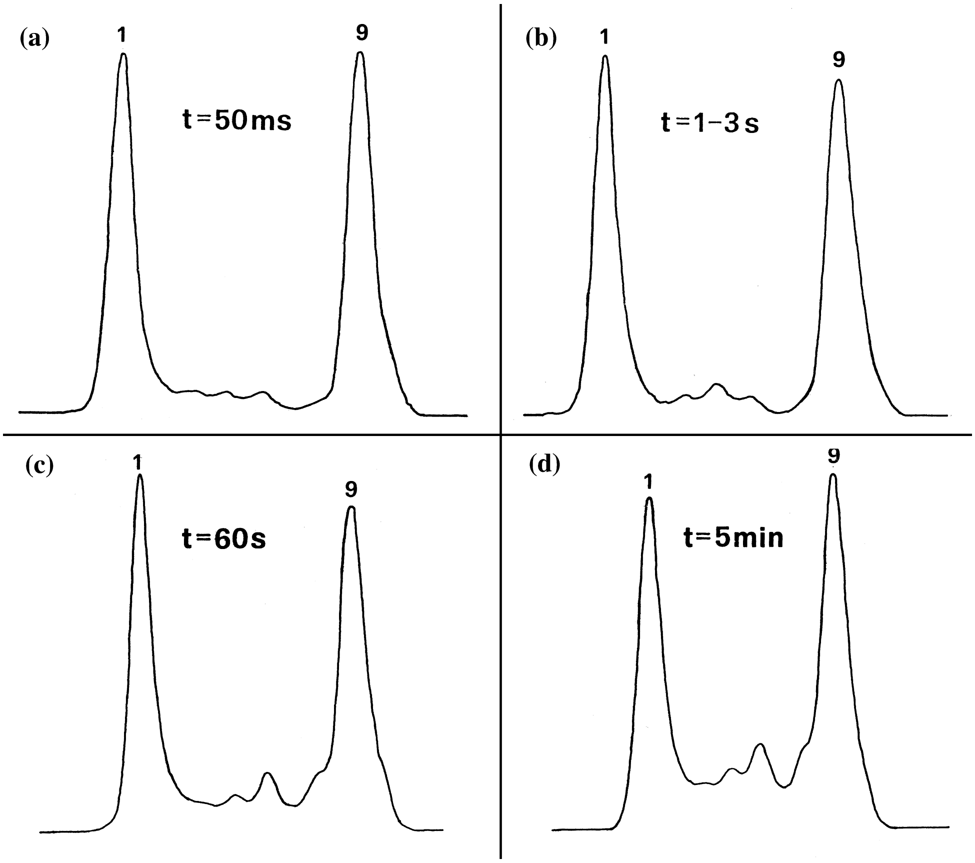

Fig. 7. Densitometer scans of colour slides of the gel tubes used for the separation by IEF at −25° of samples of 1:1 mixtures of Hb and HbCO in 0.1 M KCl, pH 7, reacted at 22° for times varying from 50 ms to 5 min before trapping the intermediates by the chemical/thermal procedure. The major peaks, labelled 1 and 9, correspond to the focused zones of Hb^+ and HbCO, respectively. Adapted from Perrella et al. [22].

8.5%; $t = 3.5$ s, $f_T = 12.3\%$; $t = 60$ s, $f_T = 21.6\%$; $t = 5$ min, $f_T = 25.4\%$; $t = 15$ min, $f_T = 24.0\%$. Such values were calculated from the densitometric scans of the color slides [22], corrected using a blank measured by the pyridine hemochromogen method. The CO saturation calculated from the mixing ratio of the reactants, 50%, agreed with that calculated from the measured fractions of the intermediates.

Fig. 8a–d are scans of color slides of gel tubes showing the approach to equilibrium in a solution of Hb containing a high proportion of intermediates [22]. The solution was obtained by mixing a sample of partially oxidised HbCO, containing approximately 37% of ferric chains, rapidly with dithionite. Dithionite reduces the ferric chains to the ferrous state restoring the functionality of the solution with regard to the CO dissociation and association reactions. After reaction times varying from 1.5 s to 15 min the solution was re-oxidised by quenching a sample into the anaerobic solution of ferricyanide cooled at −25°C. A picture of the tube of gel at reaction time $t = 0$ s, before reduction by dithionite, is shown in Fig. 6a and the scan of the colour slide of the gel in Fig. 8a. The partially oxidised species form a nearly statistical distribution since all species have the same quaternary R structure of HbCO. More than 70% of the species are valence hybrids, which yield unstable intermediates upon reduction. Under the experimental conditions the reduction of the ferric chains was completed in ≤ 1 s. At $t = 1.5$ s,

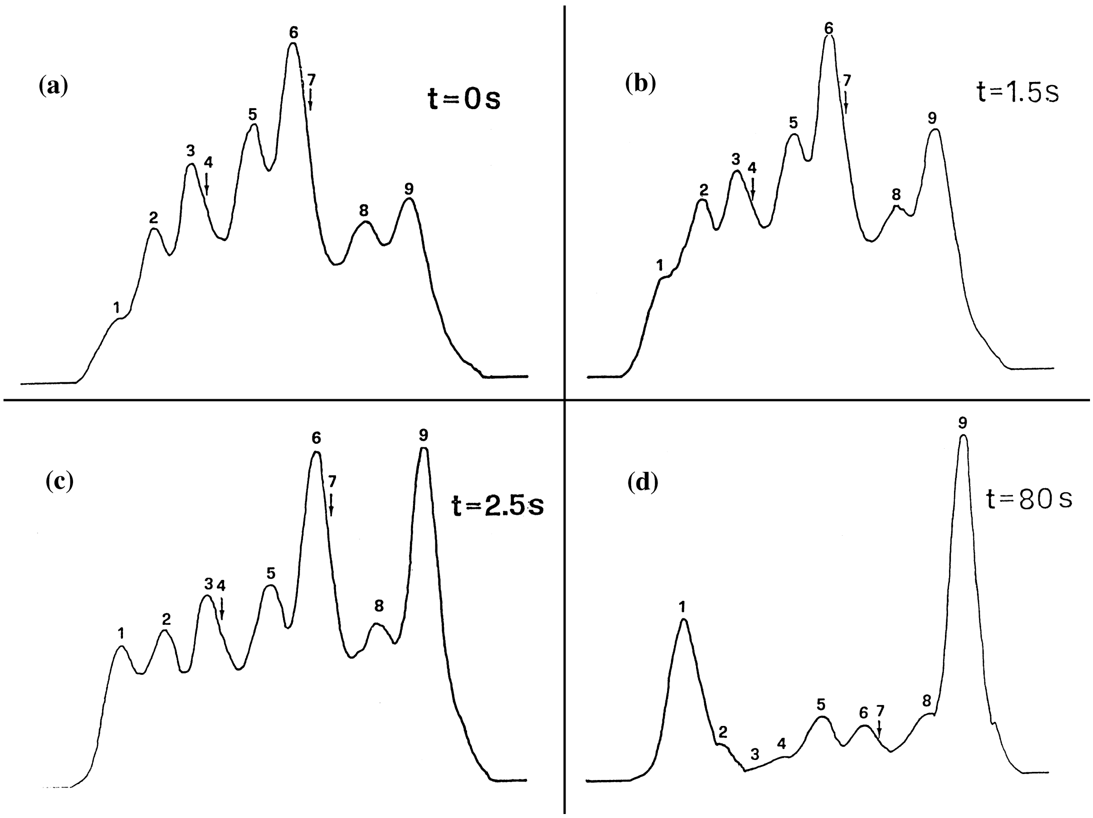

Fig. 8. (a) The distribution of species in a 37% oxidised sample of HbCO (4 mM heme concentration in 10 mM phosphate, 0.05 M KCl, pH 7) as determined by scanning a color slide of a gel tube used for focusing the sample at −25°. A picture of the gel tube with the identification of the species is shown in Fig. 6a. (b–d) Scans of color slides of gel tubes used for the separation by IEF at −25°C of the intermediates, trapped by the chemical/thermal quenching procedure and produced by reacting the 37% oxidised solution of HbCO shown in a with dithionite at 22°C for times varying from 1.5 to 80 s before quenching. Adapted from Perrella et al. [22].

Fig. 8b, a slight change in the pattern of reoxidised intermediates, with respect to the pattern in Fig. 8a, is observed, which becomes more evident at $t = 2.5$ s (Fig. 8c). At $t = 80$ s (Fig. 8d) the total fraction of intermediates had dropped from over 70% to approximately 29% of the total and was far from statistical. After 15 min the total fraction of intermediates was approximately 25%, i.e. the value reached in the approach to equilibrium experiments in Fig. 7. Such a value is also similar to the value yielded by the equilibrium concentrations listed in Table 1. The fraction of liganded chains, approximately 63%, remained constant at each reaction time indicating that the intermediates were trapped quantitatively and that the low concentrations of intermediates found after 80 s or longer were indeed the equilibrium concentrations. Fig. 8 provides both a validation of the procedure and a pictorial demonstration of cooperativity.

3. The intermediates under equilibrium conditions

An equilibrium CO isotherm was measured at 20° using concentrated hemoglobin ($\geq$ 5 g/dl) in 0.1 M KCl, pH 7.0, and CO/N_2 mixtures of known compositions [10] (Fig. 9). Under these conditions the effect of uncooperative hemoglobin dimers on the isotherm is negligible, as indicated by the value of Hill's $n = 3.4$. Furthermore, the attainment of the equilibrium between the solution and the gas phase was observed by spectroscopic and gasometric methods and the saturation values agreed with those calculated from the concentrations of the intermediates at equilibrium. More precise and detailed distributions of the intermediates under the same conditions were obtained by equilibrating various amounts of HbA and HbA(CO) in gas-tight syringes [23]. Fig. 10a shows the pattern of focused zones obtained from a nearly equimolar mixture of Hb and HbCO and Fig. 10b–c the controls carried out by quenching samples of the pure Hb and HbCO solutions. The fractions of intermediates vs. CO saturation are plotted in Fig. 11a–c. A slight chain heterogeneity is observed in the monoliganded state, which vanishes at higher saturations. The sum of the diliganded species $(\alpha\beta^{CO})(\alpha\beta^{CO})$ plus $(\alpha^{CO}\beta)(\alpha^{CO}\beta)$ is equal, within error (see also Table 1), to the sum of the diliganded species unresolved by the cryogenic technique, $(\alpha^{CO}\beta^{CO})(\alpha\beta)$ plus $(\alpha^{CO}\beta)(\alpha\beta^{CO})$. Resolution of the mixture of these intermediates, isolated at −25°, by re-focusing at 5° yielded similar concentrations of the two intermediates.

3.1. Analyses of the equilibrium distributions

Three different approaches have been used. (1) Energetics of the intermediates using the linkage between the free energies of ligand binding and of dimer assembly into tetramers, as described by Ackers and Smith [24]. (2) Site-specific thermodynamic analysis of ligand binding, as described by Di Cera [25]. (3) Comparative analyses of the

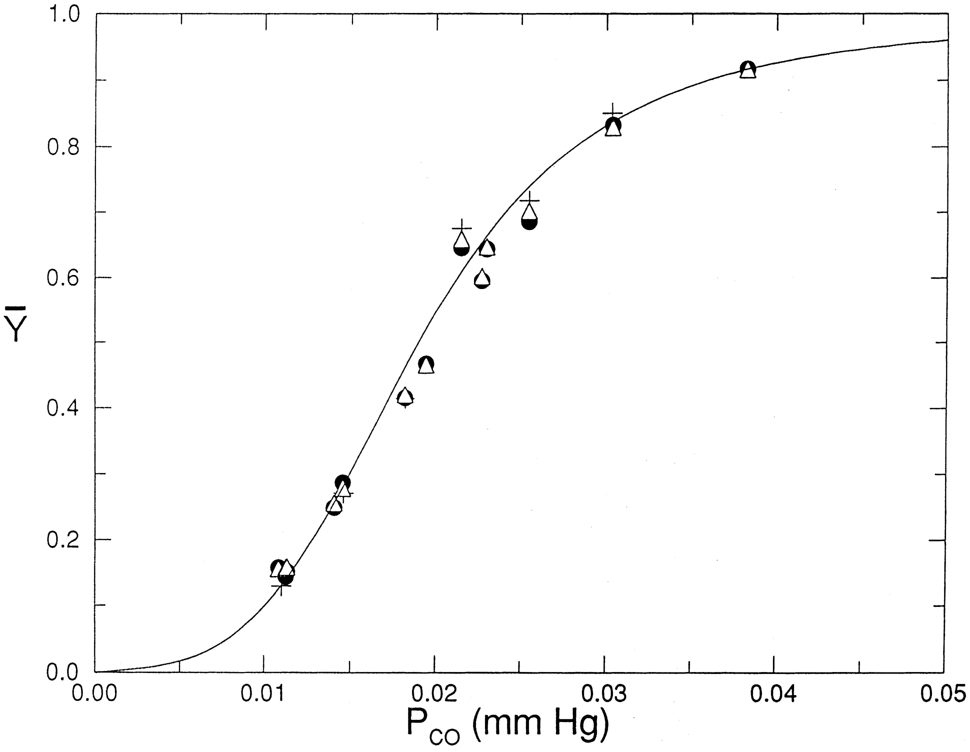

Fig. 9. Fractional CO saturation, Y, of HbA solutions (5 g dl^{-1}) in 0.1 M KCl, pH 7, equilibrated with a gas phase of varying Pco value [10]. (●) Spectrophotometric measurements. (Δ) Gas volumetric measurements. (+) Data calculated from the concentrations of the intermediates as determined in the equilibrated solutions by the chemical/thermal quenching procedure. The curve was calculated using the data on the concentrations of the intermediates. Adapted from Perrella and Denisov [15].

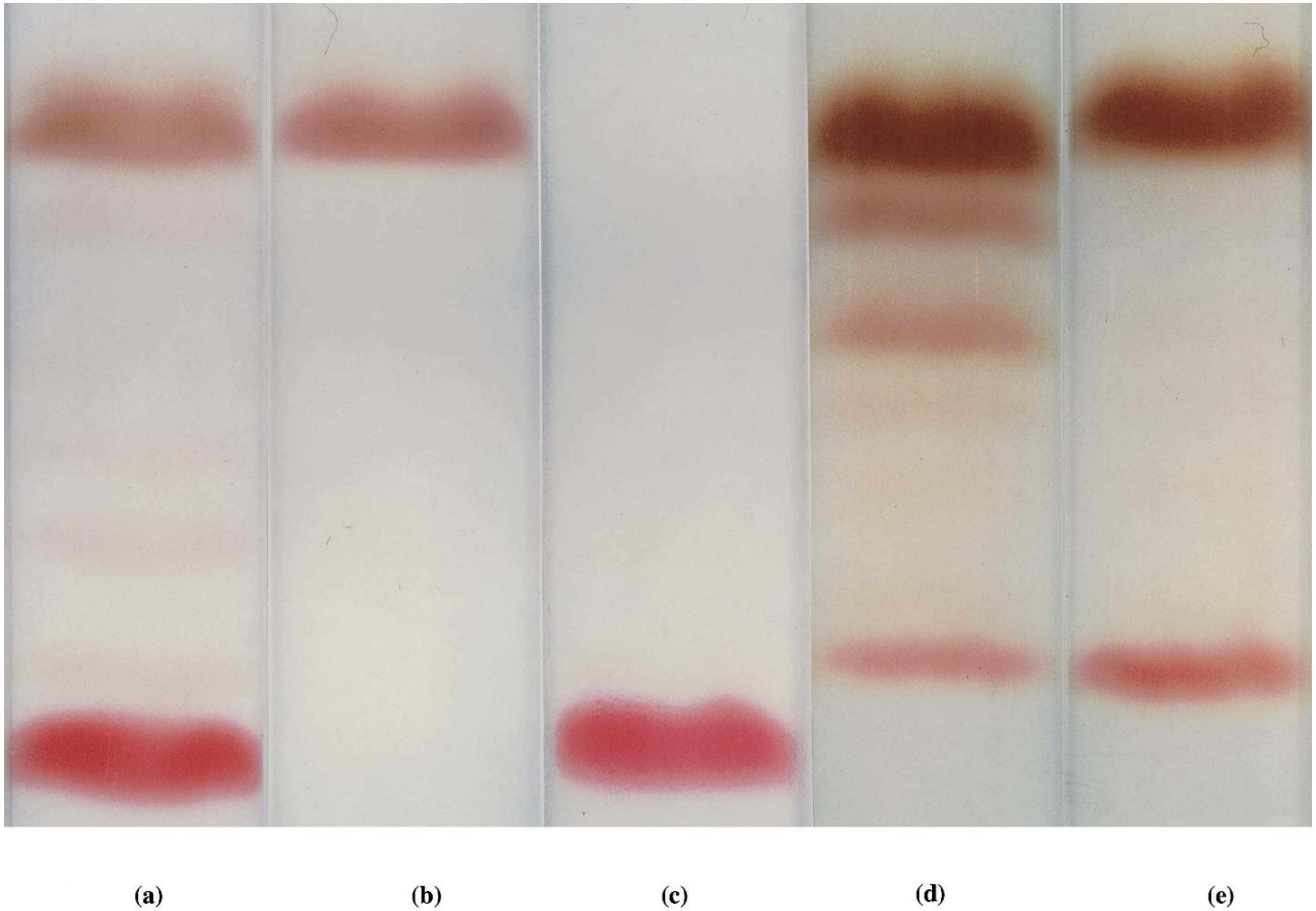

Fig. 10. Cryofocusing separations of the CO intermediates under equilibrium and dynamic conditions. (a) Pattern of intermediates in a nearly equimolar mixture of HbA and HbA(CO) in 0.1 M KCl, pH 7, equilibrated at 20°C for 20 h. (b and c) Controls carried out by quenching separately into the cryosolvent containing ferricyanide samples of pure HbA and HbA(CO), respectively. (d) Pattern of intermediates in the association reaction between HbA and CO in 0.1 M KCl, pH 7, and 20°C yielding 33% of liganded chains. (e) Control carried out by quenching samples of pure HbA and HbA(CO) into the same cryosolvent containing ferricyanide.

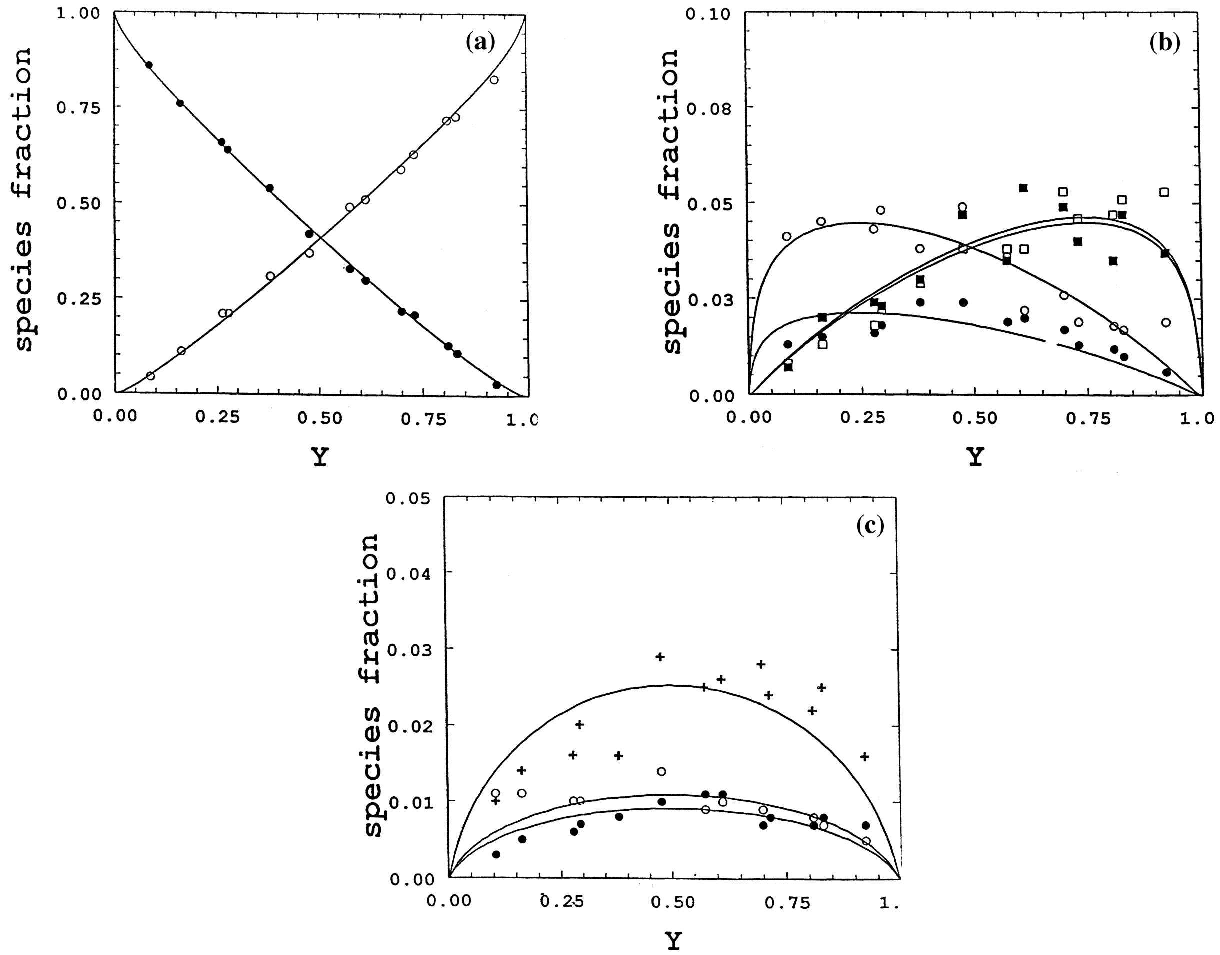

Fig. 11. Equilibrium distribution of the CO intermediates of HbA in 0.1 M KCl, pH 7, at 20°. (a) Hb (●) and HbCO (○); (b) monoliganded species $(\alpha^{CO}\beta)(\alpha\beta)$ (●), $(\alpha\beta^{CO})(\alpha\beta)$ (○), and triliganded species $(\alpha^{CO}\beta)(\alpha^{CO}\beta^{CO})$ (□), $(\alpha\beta^{CO})(\alpha^{CO}\beta^{CO})$ (■); and (c) diliganded species $(\alpha^{CO}\beta)(\alpha\beta^{CO})$ plus $(\alpha\beta)(\alpha^{CO}\beta^{CO})$ (+), $(\alpha^{CO}\beta)(\alpha^{CO}\beta)$ (●), $(\alpha\beta^{CO})(\alpha\beta^{CO})$ (○). The curves were drawn according to the site-specific partition function (Eq. (4)). Adapted from Perrella and Di Cera [23].

distributions of intermediates using a model-independent site-specific description and the MWC and KNF models [23].

3.1.1. First approach

The four equilibria between Hb and O_2 were first used by Adair to describe the binding isotherm:

$$Y=\Sigma_i iA_i[X]^i/\Sigma_i A_i[X]^i \qquad (2)$$

where Y is the fraction of liganded sites and A_i are the affinity constants, or Adair constants, between hemoglobin and i molecules of ligand X [26]. The stepwise Adair constants K_i for the consecutive binding of four molecules of ligand are related to the Adair constants A_i by the relationship: $K_i=A_i/A_{i-1}$. The Adair constants can be calculated either by a statistical analysis of the binding isotherms [27] or from the concentrations of the intermediates. The free cooperative energy of ligand binding, ΔG_C, is defined as the difference between the free energy, ΔG_{ij}, of binding i ligand molecules to a cooperative species ij, where j specifies the degeneracy of the ith ligation state (Fig. 2), and the free energy, $i\Delta G_X$, of binding i ligands to an uncooperative species, such as the hemoglobin dimers. Ackers and Smith [24] have shown that ΔG_C is also equal to the difference between the free energy, ${}^{i}\Delta G_{2j}$, of assembling uncooperative dimers to yield an ij liganded tetramer and the free energy, ${}^{0}\Delta G_{21}$, of assembling deoxy dimers into a deoxy tetramer:

$$\Delta G_c = \Delta G_{ij} - i\Delta G_x = {}^{i}\Delta G_{2j} - {}^{0}\Delta G_{21} \tag{3}$$

Eq. (3) allows one to relate the ligand affinity, A_i, to the energy of dimer assembly into tetramers, ${}^{i}\Delta G_{2j}$. At 20° in 0.1 M Cl^-, pH 7, ${}^{i}\Delta G_{2j}$ changes dramatically from the unliganded, ${}^{0}\Delta G_{21} = -14.8$ kcal mol^{-1}, to the CO liganded state, ${}^{4}\Delta G_{21} = -7.8$ kcal mol^{-1}, yielding $\Delta G_C = 7$ kcal mol^{-1}[10,11]. Therefore the ${}^{i}\Delta G_{2j}$ values of the intermediates are an important conformational probe, which can be accessed from measurements of the dimer–tetramer equilibria only for ligation models in which the mobility of the ligand is prevented. Eq. (3) allows one to obtain the ${}^{i}\Delta G_{2j}$ values of the CO intermediates from the measurements of the ligand affinities, which, in turn, can be obtained from the concentrations of the intermediates at equilibrium. Ackers and collaborators [11] have shown that in some ligation models, such as the deoxy/cyanomet hybrids, in 0.15 M chloride, pH 7.4, and 21.5°, ΔG_C for the monoliganded species and the diliganded species, $(\alpha^{+CN}\beta^{+CN})(\alpha\beta)$, is 50% of the total change from Hb to cyanomethemoglobin (HbCN). All other diliganded species and the triliganded species have the same ΔG_C value of HbCN. This finding contradicts the MWC model, which excludes the possibility that species in different states of ligation have the same energy and that species in the same state of ligation, differing for the configuration of the ligand in the tetramer, such as $(\alpha^{+CN}\beta^{+CN})(\alpha\beta)$ and $(\alpha^{+CN}\beta)(\alpha\beta^{+CN})$, have different energies. The analysis of the CO intermediates, using a non-linear least square method [28], yielded $\Delta G_C = 3.5$ kcal mol^{-1} for the monoliganded species, i.e. 50% of the total change as observed for the deoxy/cyanomet hybrids [15]. The ΔG_C value for intermediate $(\alpha^{CO}\beta^{CO})(\alpha\beta)$ could not be calculated. However, a theoretical simulation based on the estimated range of the total fraction of diliganded species, 0.5–3.5%, suggested that intermediate $(\alpha^{CO}\beta^{CO})(\alpha\beta)$ could have any value of ΔG_C in the range 7–4.5 kcal mol^{-1} [15]. The finding that the monoliganded species have a ΔG_C of 3.5 kcal mol^{-1} is consistent with the predictions of the MWC model [29]. The study failed to indicate a meaningful difference in ΔG_C value between the two key intermediates, $(\alpha^{CO}\beta^{CO})(\alpha\beta)$ and $(\alpha^{CO}\beta)(\alpha\ \beta^{CO})$, which would be inconsistent with the MWC model. Interestingly, the isotherms calculated from the concentrations of the intermediates assuming ΔG_C values for intermediate $(\alpha^{CO}\beta^{CO})(\alpha\beta)$ equal to 7 and 4.5 kcal mol^{-1}, respectively, i.e. a 20% difference, differ by less than 0.7% saturation. The values of the Hill's coefficient for the two isotherms are also almost indistinguishable [15]. These calculations point out the limitations of the traditional approaches to the study of cooperativity. The isotherms and the Hill's coefficient, although thermodynamically valid concepts, when applied to highly cooperative systems are insensitive to properties of the intermediates that are crucial for the determination of the mechanism.

3.1.2. Second approach

The partition function in Eq. (2) can be made explicit with respect to all pair-wise interactions of the chains as in Eq. (4) [30]:

$$\begin{aligned}\Sigma_i A_i[X]^i = 1 &+ 2(K_\alpha + K_\beta)[X] \\ &+ \left[c_{\alpha\alpha}K_\alpha^2 + c_{\beta\beta}K_\beta^2 \right.\\ &\left. + 2(c_{\alpha\beta} + c'_{\alpha\beta})K_\alpha K_\beta\right][X]^2 \\ &+ 2(c_{\alpha\alpha\beta}K_\alpha + c_{\alpha\beta\beta}K_\beta)K_\alpha K_\beta[X]^3 \\ &+ c_{\alpha\alpha\beta\beta}K_\alpha^2 K_\beta^2[X]^4\end{aligned} \tag{4}$$

where K_α and K_β are the affinities of the two chains in the unliganded state and c's are the pair-wise coupling constants, which define either the cooperative nature of the chain interactions or the absence of cooperativity. Because of the non-equivalence of intermediates $(\alpha^{CO}\beta^{CO})(\alpha\beta)$ and $(\alpha^{CO}\beta)(\alpha\beta^{CO})$, $c_{\alpha\beta}$ and $c'_{\alpha\beta}$ can have equal or different values. Di Cera [30] has provided the solution of the partition function and calculated the values of the *c*'s for the distribution of CO intermediates at 48% saturation listed in Table 1. From such values the free energies for the interactions of each pair of liganded chains as a function of the state of ligation of the remaining two chains were calculated, i.e. ΔG_{00} in the case of no ligation, ΔG_{10} and ΔG_{01} in the case of one liganded chain, and ΔG_{11} if both chains are liganded. The energy values listed in Table 2 were calculated assuming $c_{\alpha\beta} = c'_{\alpha\beta}$. Listed in Table 2 are also the values calculated assuming the MWC model, which predicts an energy minimum at 50% saturation. The free energies are negative, indicating that all interactions produce positive cooperativity, and are, within error, equal in value, i.e. they are independent of the interacting chains and of the saturation.

The calculations carried out assuming $c_{\alpha\beta} = 20 \times c'_{\alpha\beta}$ yielded a similar picture. In either case the energy values do not conform to the prediction of the MWC model and are the expression of a mechanism following the rules of the KNF model [30]. The energy values calculated using the data on the concentrations of the intermediates in the low and high CO saturation ranges were similar to those obtained at 50% saturation (Di Cera, personal communication).

3.1.3. Third approach

The concentrations of the intermediates vs. CO saturation in Fig. 11 were fitted using the model-independent site-specific Eq. (4) and the binding equations derived for the MWC and KNF models [30]. The lines in Fig. 11 are the result of the site-specific analysis. The affinities calculated for the three cases, listed in Table 3, are significantly different. The MWC model markedly underestimates the nearly 10-fold increase in affinity from the first to the second ligation state evidenced by the model-independent analysis. The values of the *cs* derived for the model-independent analysis indicate strong chain interactions throughout the ligation process (see Table 1). The MWC and KNF models fit the experimental data similarly, but less satisfactorily than the site-specific analysis. Both underestimate the population of diliganded species, particularly the MWC model, which yields a value of 1% at 50% saturation against the experimental value of approximately 5% (Table 1). This finding indicates that a good qualitative agreement between the distributions of intermediates at equilibrium calculated by a model-dependent analysis of kinetic data and the experimental data obtained by the cryogenic technique is not sufficient to exclude other models [31].

Despite the significant discrepancies in the values of the affinity constants derived from the three types of analysis the calculated isotherms cannot be distinguished (Fig. 12). This confirms the inadequacy of the analyses of isotherms for the study of mechanisms, as noted above, and, in particular, for discriminating models of cooperativity.

4. Intermediates under dynamic conditions

The association reaction between hemoglobin and CO and the effects of several modulators on

Table 2
Free energies of pairwise chain interactions (kcal mol^{-1}) for CO binding to hemoglobin calculated from the data in Table 1, adapted from Di Cera [30]

Pair	ΔG_{00}	ΔG_{10}	ΔG_{01}	ΔG_{11}
$c_{\alpha\beta} = c_{\alpha\beta} = 10.5$				
$\alpha_1\ \alpha_2$	-2.0 ± 0.2	-1.2 ± 0.2	-1.2 ± 0.2	-1.3 ± 0.2
$\alpha_1\ \beta_1$	-1.4 ± 0.2	-0.7 ± 0.2	-1.0 ± 0.2	-1.0 ± 0.2
$\alpha_1\ \beta_2$	-1.4 ± 0.2	-0.7 ± 0.2	-1.0 ± 0.2	-1.0 ± 0.02
$\beta_1\ \beta_2$	-1.3 ± 0.2	-1.0 ± 0.2	-1.0 ± 0.2	-1.3 ± 0.2
MWC	-0.5	-2.6	-2.6	-0.3

Table 3
The stepwise Adair constants K_i ($i = 1$–4) (torr^{-1}) calculated from the equilibrium distributions of CO intermediates according to a model in-site-specific analysis and to the MWC and KNF models [23]

Site-specific analysis	MWC model	KNF model
$K_1 = 1.7 \pm 0.2$	$K_1 = 2.0 \pm 0.2$	$K_1 = 2.2 \pm 0.2$
$K_2 = 28 \pm 2$	$K_2 = 5.9 \pm 0.6$	$K_2 = 18 \pm 1$
$K_3 = (1.3 \pm 0.1) \times 10^2$	$K_3 = (6.1 \pm 0.7) \times 10^2$	$K_3 = (1.4 \pm 0.1) \times 10^2$
$K_4 = (1.0 \pm 0.1) \times 10^3$	$K_4 = (9.1 \pm 0.9) \times 10^2$	$K_4 = (1.2 \pm 0.1) \times 10^3$

the reaction were studied by the isolation of the intermediates formed when Hb reacts with substoichiometric amounts of CO (Fig. 10d,e and Fig. 13) [19,32]. The lines fitting the distributions of intermediates at different pH values in Fig. 13 were obtained by numerical methods using a simplified kinetic scheme of four consecutive reactions, which does not distinguish intermediates in the same state of ligation [33]. This approach yields only relative values of the rate constants, which, however, is the relevant piece of information for the study of the cooperative mechanism of the binding reaction. The rate constants for the association reaction, as obtained from the analyses of the distributions of intermediates at different pH values in 0.1 M KCl, reveal that the reaction is cooperative at each binding step under all conditions. The overall cooperativity, as measured by the ratio of the rate constants between the last and first reaction, l'_4/l'_1, and the acceleration in the reaction, as measured by the ratio of the constants between any two consecutive reactions, l'_n/l'_{n-1}, are pH-dependent, Table 4 [19]. At pH 6.3, $l'_4/l'_1 = 22$ and a significant acceleration is observed after the binding of the third ligand. At pH 7, $l'_4/l'_1 = 53$ and an acceleration is observed after the binding of the second ligand. At pH 8.5, $l'_4/l'_1 = 67$ and an acceleration is observed after the binding of the first ligand. Because of the complexity of the kinetics this behaviour could not be predicted by the classical flow kinetics work of Gibson et al. [34,35].

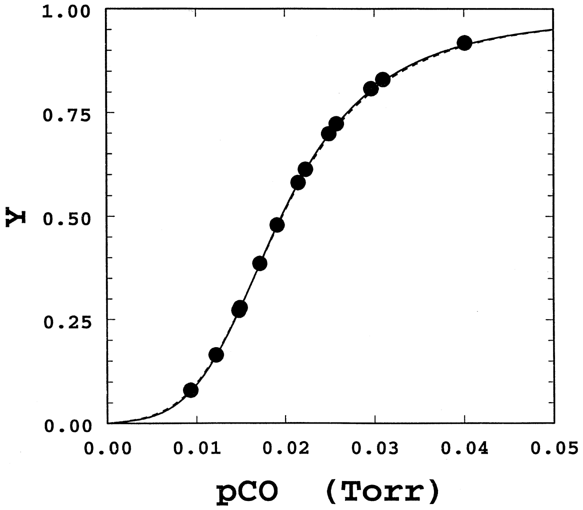

Fig. 12. (●) CO fractional saturation values calculated from the distributions of intermediates in Fig. 11. Also shown are the curves obtained from the affinity constants derived from analyses of the intermediates using the MWC (continuous line) and KNF (dashed line) models.

Table 4
Ratios l'_n/l'_{n-1} and l'_4/l'_1 of the stepwise rate constants for the CO association reaction at 20° in 0.1 M KCl and different pH values according to a mechanism of four consecutive reactions [19]

	pH		
	6.3	7.0	8.5
l'_2/l'_1	1.89 ± 0.23	2.34 ± 0.32	9.66 ± 1.31
l'_3/l'_2	2.70 ± 0.36	5.55 ± 0.84	1.98 ± 0.31
l'_4/l'_3	4.30 ± 0.43	4.08 ± 0.47	3.53 ± 0.41
l'_4/l'_1	22.0 ± 1.8	53.1 ± 5.2	67.6 ± 6.1

Another feature of the association reaction clarified by the cryogenic method is the slight functional heterogeneity of the chains, particularly in the first binding step. This aspect of the CO kinetics, and its structural interpretation, has been controversial, but it has been recently confirmed by the stopped-flow studies of native and mutant hemoglobin of Olson et al. [36,37]. Chain heterogeneity is slight, but significant, and is influenced by pH, chloride at neutral pH, and inositolhexaphosphate (IHP) [19,32]. Particularly interesting is the effect of IHP [32]. In 0.1 M chloride, pH 7, CO binds to the β chains first. The addition of IHP in 2:1 ratio with Hb reverses the order of reactivity of the chains, although the overall rate of the association reaction is not affected significantly. This suggests that IHP binding to the β chains modifies the rate of the reaction with CO not only of the β chains, but also of the α chains. The implications are that the MWC interpretation of the effect of the modulators as due to the stabilisation of the T structure may be an oversimplification of the mechanism and, possibly, that mechanisms may exist for the interaction among the modulators other than the simple competition for the same binding site, as indicated by the experiments in Fig. 1.

The data at different pH values in 0.1 M KCl are compared in Fig. 14 with the distributions of intermediates predicted by a kinetic form of the MWC model, which assumes an instantaneous equilibration between the T and R structures of the intermediates at each ligation step [19]. The fractions of molecules in the T and R structures were calculated using data from the O_2 binding isotherms as measured at different pH values by Imai [38] and by Chu et al. [39]. The poor agreement between the predictions of the MWC model and the experimental data at acidic and neutral pH could be due to the approximations of the kinetic model. At alkaline pH, however, the large deviation from the prediction of the MWC model suggests that cooperativity in the association reaction does not ensue solely from quaternary changes in structure.

5. Conclusions

The cryogenic technique for trapping the intermediates in the reactions of hemoglobin with CO has disclosed features of the mechanism of cooperativity in this paradigmatic protein that could not be revealed by the study of the bulk properties of hemoglobin solutions either under equilibrium or dynamic conditions. Carbon monoxide is the closest approximation to the physiological ligand that is available for study by the cryogenic technique at present. How far the information obtained from these studies can be extrapolated to oxygen may be questionable because of the known differences in chemical bonding to the heme between O_2 and CO and the different stereochemical constraints imposed by the heme pocket on the binding of the two ligands. ^{1}H-NMR studies by Ho et al. have revealed heterogeneity of the chains in hemoglobin solutions in equilibrium with O_2 in the presence of organic phosphate [40,41]. The higher affinity for O_2 of the α chains as compared to that of the β chains under these conditions is paralleled by the preferential CO binding to the α chains observed by the cryogenic technique in the presence of IHP under dynamic conditions [32]. This suggests that at least some of the mechanistic information obtained with CO can be qualitatively extrapolated to the physiological ligand. In a recent study of the kinetics of oxygen binding to hemoglobin Gibson [42] reached the conclusion that a simple two-state model is not adequate to describe the oxygen interactions.

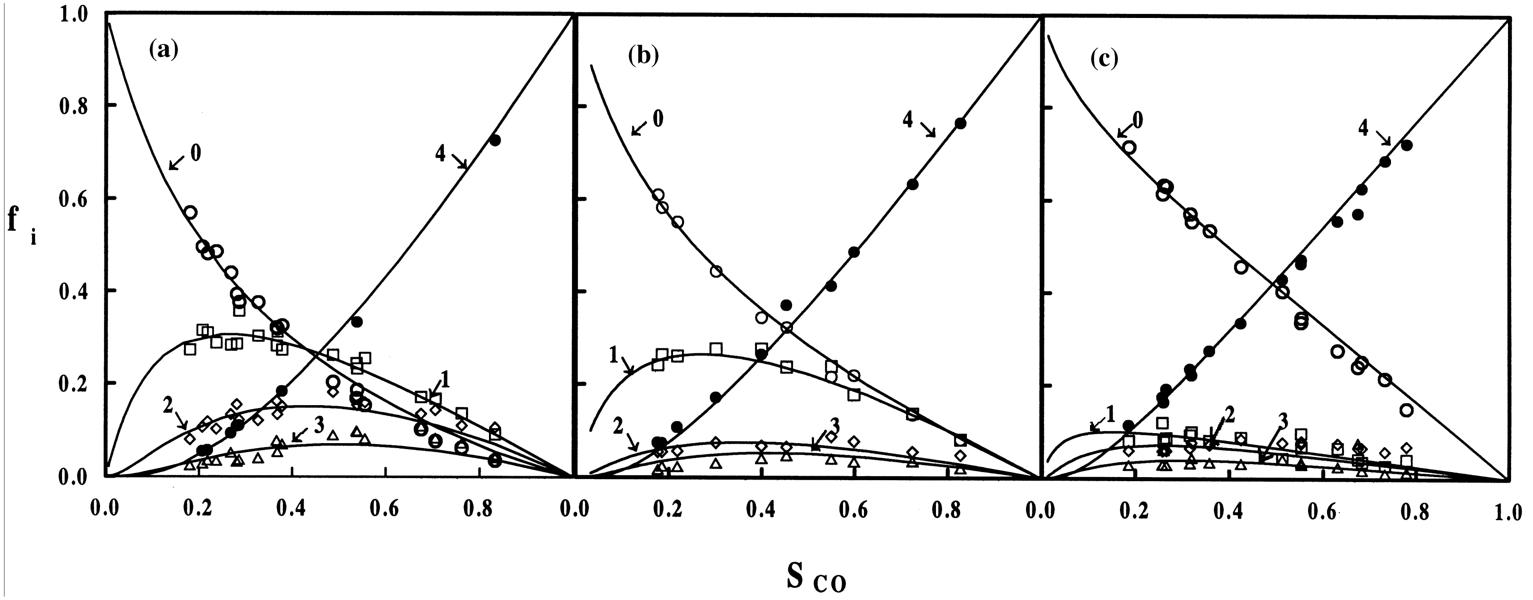

Fig. 13. Fractional values, f_i, of the concentrations of the species formed in the association reaction between HbA and CO at 20°C vs. total fractional value of bound CO, S_{CO}. Hb, (○); HbCO, (●); sum of monoliganded intermediates, (□); sum of diliganded intermediates, (◇); sum of triliganded intermediates, (Δ). (A) Pooled data at pH 6.3 in 7 and 100 mM KCl [19]. (B) Data at pH 7.0 in 100 mM KCl [32]. (C) Pooled data at pH 8.5 in 7 and 100 mM KCl [19]. Lines fitted according to a four rate constant scheme of consecutive reactions, l'_1, l'_2, l'_3, l'_4, assuming $l'_4 = 6.0\ \mu M^{-1}\ s^{-1}$ under all conditions [35]. The state of ligation of the intermediates for each line is indicated by the respective arrows.

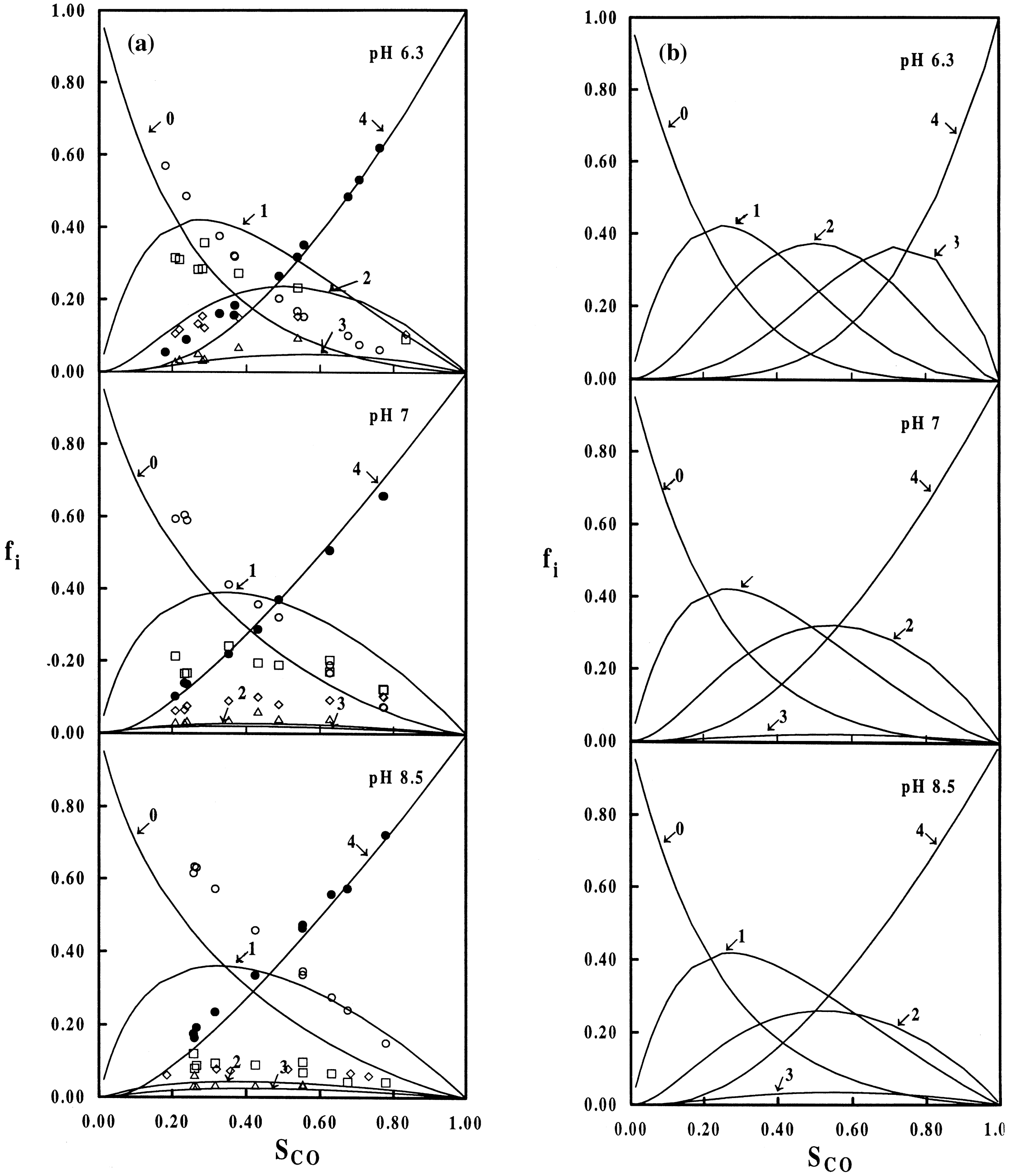

Fig. 14. Distributions of intermediates (full lines) generated in the association reaction between HbA and CO at 20° in 100 mM KCl and pH 6.3, 7.0 and 8.5, as calculated assuming concerted transitions of quaternary structures at each ligation step. Calculations based on the values of the allosteric constant *L* determined by Imai [38] (A) and by Chu and Ackers [39] (B). In panel (A) the concentrations of intermediates, as obtained at the same pH values and shown in Fig. 13, are added for comparison. Symbols as in Fig. 13. Adapted from Perrella et al. [19].

The analyses of the distributions of the intermediates have demonstrated that the binding isotherms, although thermodynamically valid concepts, are inadequate tools for the study of the mechanisms in highly cooperative systems. Direct information on the intermediates is mandatory. The limitation of the cryogenic technique, which resolves only nine out of the 10 species reacting with CO, has been overcome, as described above [19]. The differences in the functional properties of species $(\alpha^{CO}\beta^{CO})(\alpha\beta)$ and $(\alpha^{CO}\beta)(\alpha\ \beta^{CO})$ are very slight, as indicated by the similarity of their concentrations under dynamic and equilibrium conditions. Because of their paucity the precision in the determination of these key intermediates is still inadequate to answer a crucial question. The mechanism proposed by Ackers [43], known as the symmetry rule, suggests that intermediates $(\alpha^L\beta^L)(\alpha\beta)$ and $(\alpha^L\beta)(\alpha\beta^L)$ are in the T and R quaternary structures, respectively, thereby having significantly different functional properties. This mechanism implies that tertiary structural changes in the hemoglobin dimeric unit within the T structure contribute partly to cooperativity. It may be over-demanding on the cryogenic technique, at the present state of the art, to ask if such a requirement is also fulfilled for the case of $L = \mathrm{CO}$. The physiological significance of the discrepancy between the similarity in the properties of intermediates $(\alpha^L\beta^L)(\alpha\beta)$ and $(\alpha^L\beta)(\alpha\beta^L)$ when L is CO and the marked difference observed in other ligation models by Ackers et al. [11], is that a large functional heterogeneity in these intermediates, if occurring also with O_2, would suppress cooperativity and impair oxygen transport [15]. The discrepancy among different ligation models should not be overemphasised. More intriguing are the structural reasons responsible for the observed energetic plasticity of the intermediates. The main general conclusion reached by the work on the CO intermediates, both under dynamic and equilibrium conditions, is that cooperativity ensues from tertiary and quaternary structural changes. This is not a requirement of the classical formulation of the MWC model and is also the major novelty of the symmetry rule.

Acknowledgements

This work was supported by a grant from MURST. I am grateful to various collaborators, in particular L. Benazzi and M. Ripamonti. Various technical difficulties were overcome with the help of R.L. Berger. I am most indebted to Gary Ackers for his appreciation for the work I have undertaken, his encouragement and the many fruitful and illuminating discussions.

References

[1] M.F. Perutz, Mechanisms of cooperativity and allosteric regulation in proteins, Q Rev Biophys 22 (1989) 139–236.

[2] R.E. Dickerson, I. Geis, Hemoglobin: Structure, Function, Evolution and Pathology, Benjamin/Cummings, Menlo Park, 1983.

[3] J.V. Kilmartin, L. Rossi-Bernardi, Interaction of hemoglobin with hydrogenions, carbon dioxide, and organic phosphates, Physiol Rev 53 (1973) 836–890.

[4] O. Brenna, M. Luzzana, M. Pace, M. Perrella, F. Rossi, L. Rossi-Bernardi, F.J.W. Roughton, The interaction between hemoglobin and its 'oxygen-linked' ligands, in: hemoglobin and red cell structure and function, in: G.J. Brewer (Ed.), Advances in Experimental Medicine and Biology, 28, Plenum Press, New York, 1972, pp. 19–40.

[5] J. Monod, J. Wyman, J.P. Changeaux, On the nature of allosteric transitions: a plausible model, J Mol Biol 12 (1965) 88–118.

[6] D.E. Koshland, G. Nemethy, D. Filmer, Comparison of experimental binding data and theoretical models in proteins containing subunits, Biochemistry 5 (1966) 365–385.

[7] J.S. Olson, Stopped-flow, rapid mixing measurements of ligand binding to hemoglobin and red cells, Methods Enzymol 76 (1981) 631–651.

[8] M. Samaja, E. Rovida, M. Niggeler, M. Perrella, L. Rossi-Bernardi, The dissociation of carbon monoxide from hemoglobin intermediates, J Biol Chem 262 (1987) 4528–4533.

[9] E. Di Cera, M.L. Doyle, P.R. Connelly, S.J. Gill, Carbon monoxide binding to human hemoglobin A0, Biochemistry 26 (1987) 6494–6502.

[10] M. Perrella, A. Colosimo, L. Benazzi, M. Ripamonti, L. Rossi-Bernardi, What the intermediate compounds in ligand binding to hemoglobin tell about the mechanism of cooperativity, Biophys Chem 37 (1990) 211–223.

[11] G.K. Ackers, Deciphering the molecular code of hemoglobin allostery, Adv Protein Chem 51 (1998) 185–253.

[12] P. Douzou, Cryobiochemistry, Academic Press, New York, 1977.

[13] C.M. Park, Isoelectric focusing and the study of interacting protein systems: ligand binding, phosphate binding,

and subunit exchange in hemoglobin, Ann NY Acad Sci 209 (1973) 237–258.

[14] M. Perrella, L. Rossi-Bernardi, Detection of hemoglobin hybrid formation at subzero temperature, Methods Enzymol 76 (1981) 133–143.

[15] M. Perrella, I. Denisov, Low temperature electrophoresis methods, Methods Enzymol 259 (1995) 468–487.

[16] M. Perrella, M. Samaja, L. Rossi-Bernardi, Hybrid formation for liganded hemoglobins A and C at subzero temperatures, J Biol Chem 254 (1979) 8748–8750.

[17] M. Perrella, L. Cremonesi, I. Vannini Parenti, L. Benazzi, L. Rossi-Bernardi, paH gradients in isoelectric focusing experiments at subzero temperatures, Anal Biochem 105 (1980) 126–132.

[18] M. Perrella, L. Cremonesi, L. Benazzi, L. Rossi-Bernardi, Isolation of intermediate valence hybrids between ferrous and methemoglobin at subzero temperatures, J Biol Chem 256 (1981) 11098–11103.

[19] M. Perrella, M. Ripamonti, S. Caccia, Modulation of the association reaction between hemoglobin and carbon monoxide by hydrogenion and chloride, Biochemistry 37 (1998) 2017–2028.

[20] V.J. LiCata, P.C. Speros, E. Rovida, G.K. Ackers, Direct and indirect pathways of functional coupling in human hemoglobin are revealed by quantitative low-temperature isoelectric focusing of mutant hybrids, Biochemistry 29 (1990) 9771–9783.

[21] M. Perrella, L. Rossi-Bernardi, Hemoglobin liganded intermediates, Methods Enzymol 232 (1994) 445–460.

[22] M. Perrella, L. Sabbioneda, M. Samaja, L. Rossi-Bernardi, The intermediate compounds between human hemoglobin and carbon monoxide at equilibrium and during approach to equilibrium, J Biol Chem 261 (1986) 8391–8396.

[23] M. Perrella, E. Di Cera, CO ligation intermediates and the mechanism of hemoglobin cooperativity, J Biol Chem 274 (1999) 2605–2608.

[24] G.K. Ackers, F.R. Smith, The hemoglobin tetramer: a three-state molecular switch for control of ligand affinity, Annu Rev Biophys Biophys Chem 16 (1987) 583–609.

[25] E. Di Cera, Thermodynamics of local linkage effects. Contracted partition functions and analysis of site-specific energetics, Biophys Chem 37 (1990) 147–164.

[26] G.S. Adair, The hemoglobin system. VI. The oxygen dissociation curve of hemoglobin, J Biol Chem 63 (1925) 529–545.

[27] M.L. Doyle, D.W. Myers, G.K. Ackers, R.I. Shrager, Weighted nonlinear regression analysis of highly cooperative oxygen equilibrium curves, Methods Enzymol 232 (1994) 576–597.

[28] M.L. Johnson, Evaluation and propagation of confidence intervals in non-linear asymmetrical variance space. Analysis of ligand binding data, Biophys J 44 (1983) 101–106.

[29] G.K. Ackers, M.L. Johnson, Linked functions in allosteric proteins. Extension of the concerted (MWC) model for oxygen-linked subunit assembly and its application to human hemoglobin, J Mol Biol 147 (1981) 559–582.

[30] E. Di Cera, Thermodynamic Theory of Site-Specific Binding Processes in Biological Macromolecules, Cambridge University Press, Cambridge, 1995.

[31] E.R. Henry, C.M. Jones, J. Hofrichter, W.A. Eaton, Can a two-state MWC allosteric model explain hemoglobin kinetics? Biochemistry 36 (1997) 6511–6528.

[32] M. Perrella, N. Davids, L. Rossi-Bernardi, The association reaction between hemoglobin and carbon monoxide as studied by the isolation of the intermediates, J Biol Chem 267 (1992) 8744–8751.

[33] R.L. Berger, N. Davids, M. Perrella, Simulation of hemoglobin kinetics using finite element numerical methods, Methods Enzymol 232 (1994) 517–530.

[34] Q.H. Gibson, The kinetics of reactions between hemoglobin and gases, Prog Biophys Biophys Chem 9 (1959) 1–53.

[35] R. Mac Quarry, Q.H. Gibson, Ligand binding and release of an analogue of 2,3-biphosphoglycerate from human hemoglobin, J Biol Chem 247 (1972) 5686–5694.

[36] A.J. Mathews, J.S. Olson, J.P. Renaud, J. Tame, K. Nagai, The assignment of carbon monoxide association rate constants to the alpha and beta subunits in native and mutant deoxyhemoglobin tetramers, J Biol Chem 266 (1991) 21631–21639.

[37] A.J. Mathews, J.S. Olson, Assignment of rate constants for O_2 and CO binding to α and β subunits within R- and T-state human hemoglobin, Methods Enzymol 232 (1994) 363–386.

[38] K. Imai, Allosteric Effects in Hemoglobin, Cambridge University Press, Cambridge, 1982.

[39] A.H. Chu, B.W. Turner, G.K. Ackers, Effects of hydrogen ions on the deoxygenation-linked subunit assembly in human hemoglobin, Biochemistry 23 (1984) 604–617.

[40] M.E. Johnson, C. Ho, Effects of ligands and organic phosphates on functional properties of human adult hemoglobin, Biochemistry 13 (1974) 3653–3660.

[41] G. Viggiano, C. Ho, Hydrogen ion nuclear magnetic resonance investigation of structural changes associated with cooperative oxygenation of human adult hemoglobin, Proc Natl Acad Sci USA 76 (1979) 3673–3677.

[42] Q.H. Gibson, Kinetics of oxygen binding to hemoglobin A, Biochemistry 38 (1999) 5191–5199.

[43] G.K. Ackers, M.L. Doyle, D. Myers, M.A. Daugherty, Molecular code for cooperativity in hemoglobin, Science 255 (1992) 54–63.